The Abdus Salam International Centre for Theoretical Physics

United Nations Educational, Scientific and Cultural Organization

IAEA

1965-33

9th Workshop on Three-Dimensional Modelling of Seismic Waves Generation, Propagation and their Inversion

22 September - 4 October, 2008

The study of fluid-induced and triggered seismicity: case studies Part II

Torsten Dahm

Institut für Geophysik
Universität Hamburg
Germany

torsten.dahm@zmaw.de

The study of fluid-induced and triggered seismicity: case studies

ICTP Course 2008

Torsten Dahm

torsten.dahm@zmaw.de

Institut für Geophysik, Universität Hamburg, Germany

Contributions from:
G. Manthei, M. Hensch, E. Rivalta, J. Reinhardt, Th. Fischer

Examples

1. Fluid injection and pore pressure diffusion
2. Hydro-fracturing & magma intrusions
   - Gas field stimulation
   - Long lasting intrusions
3. Gas field depletion

Case I: fluid & pore pressure diffusion

Examples:

– Denver 1962-1968: three M>5 events, 21 month after the end of injection

– Chalia chemical waste disposal 1972-1985, M5 event 12 km south of well 14 years after injection

– Ashtabula, Ohio, sequence 1987-2003, M< 4.3, 9 years after end of injection

References for all three cases given in Seeber et al. (2004)

Example: Temperature-diffusion in salt mine

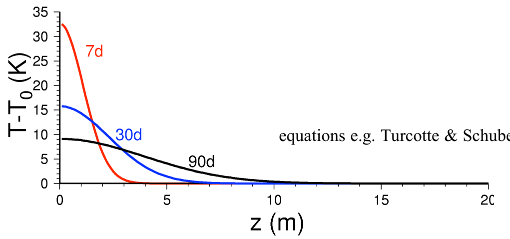

equations e.g. Turcotte & Schubert(2002)

1-D Temperature diffusion after "heat injection" at plane z=0.

Temperature (and stress) slowly spreads out and "relaxes" at "injection point"

The same laws apply for fluid and pore pressure diffusion or dissolution

The Ashtabula, Ohio, sequence related to waste fluid injection

into 1.8 km deep sandstone

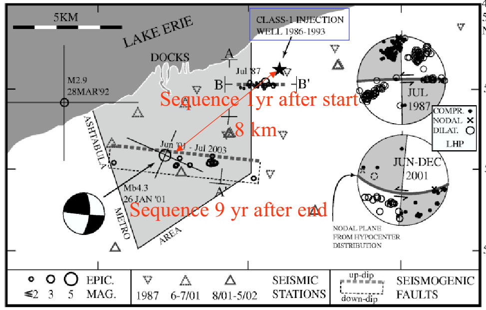

Hypo depth in basement 2 km below the injection layer

Seeber at al., 2004, BSSA 94, 76-87

Temporal evolution

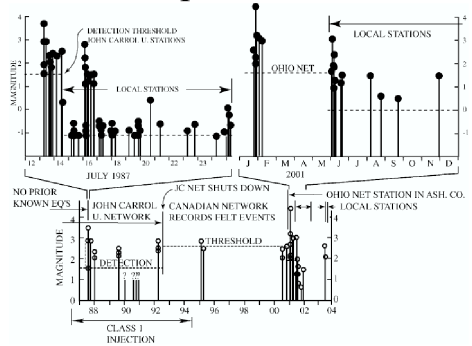

164 m^3/day at 10 MPa (59.860 tons/yr) Seeber at al., 2004, BSSA 94, 76-87

Compare: planned CO_2 sequestration intends to inject several Mt / yr over >15 yr

Fluid-injection triggered events

1. Injection related pore pressure rise (diffusive) triggers earthquakes according to Coulomb criterion
2. Pore pressure dropping back at the well after injection stops, but maximum continuous to spread away from injection well for tens of years up to 8 - 14 km distance or more
3. Pore pressure transients can be simulated by hydraulic diffusive modelling

Case II

Hydrofracture induced seismicity

Hydrofrac stimulations in Canyonsand gas field, W. Texas

injection borehole

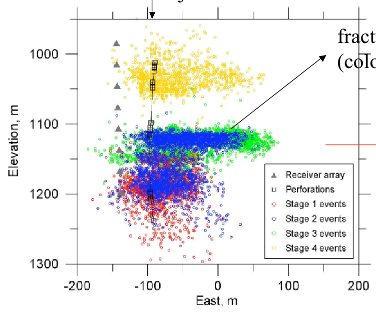

fracture-induced seismicity (color = different experiments)

growth direction (2D)

Fischer et al. (JGR, 2008)

distance time plot, stage 3

growth direction

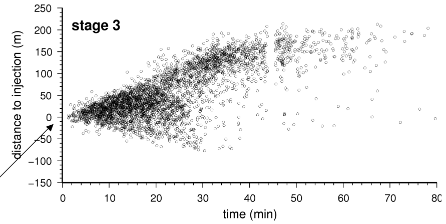

injection point

09/23/08

distance time plot, stage 3

t1 t2 t3 t4

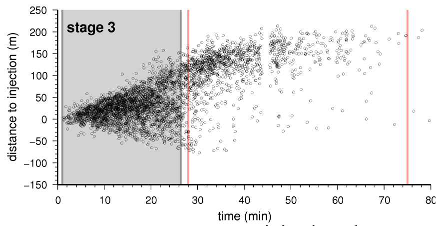

injection phase

post-injection phase

09/23/08

distance time plot, stage 3

max. length

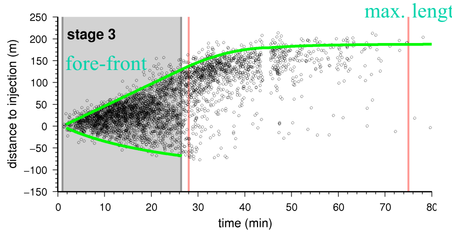

09/23/08

distance time plot, stage 3

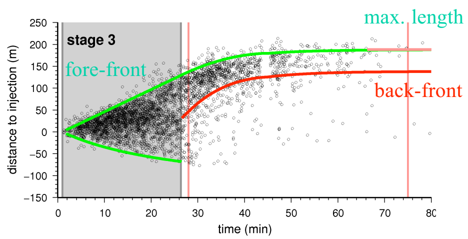

09/23/08

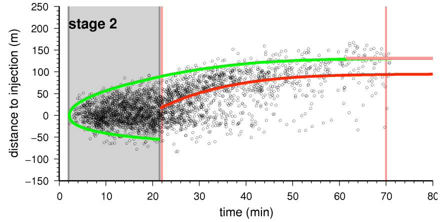

Hypotheses:

a) Front and backfront are controlled by pressure diffusion

b) Front- and backfront, asymmetric growth and intensity of seismicity are controlled by the shape of the fluid-filled fracture (our model)

09/23/08

Sketch of hydrofracture

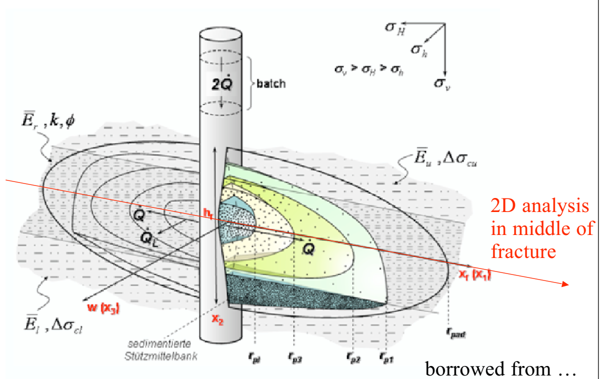

borrowed from …

Fracture opening during injection

without gradient

with stress gradient

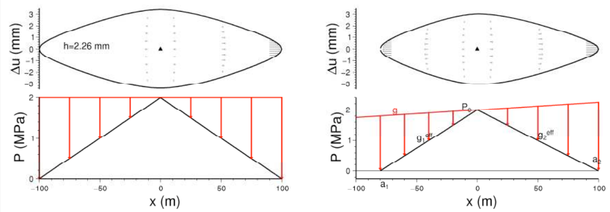

Injection pressure P0 and gradient g controls growing velocity

09/23/08

Injection phase: driving pressure and flow

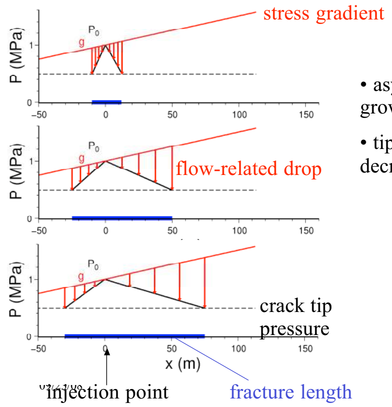

- asymmetric bilateral growth
- tip grow velocity decreasing with length

Dahm et al., 2008

After injection: self-expanding bilateral growth

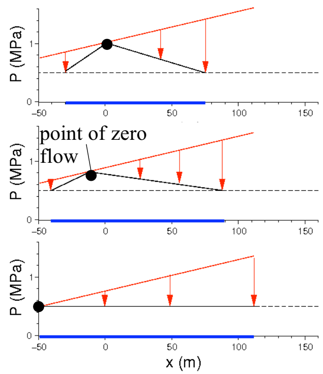

- bilateral growth with decreasing velocity
- decreasing ambient overpressure
- point of "zero flow" is moving backward towards taller tip

Dahm et al., 2008

self-expanding unilateral growth

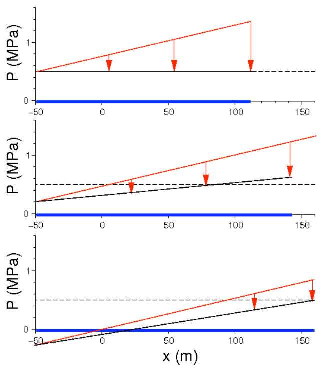

- unilateral growth
- ambient overpressure is further decreasing
- overpressure at taller tip is decreasing below critical value
- at final stage the overpressure at taller tip is below zero (Weertman crack)

09/23/08

Dahm et al., 2008

shape of the unilateral self-expanding crack

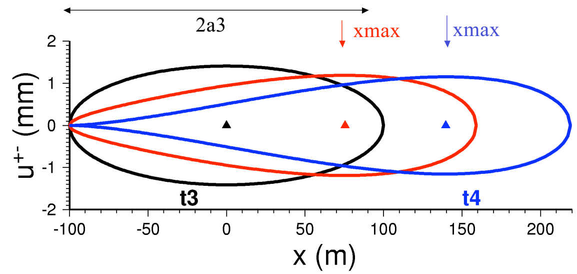

The total fluid volume is constant.

Final length at time t4 is 1.59 the initial length.

Point of max. opening defines the back-front of seismicity

09/23/08

Dahm et al., 2008

rate of maximal induced shear stress

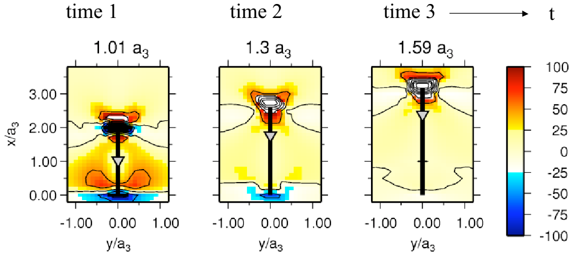

Regions of increasing shear stress have higher trigger potential.
Modeling confirms the behavior of front and back-front

2D boundary element method (100 elements) considering theoretical pressure distribution and elastic full space

09/23/08

Dahm et al., 2008

Fit to seismicity data

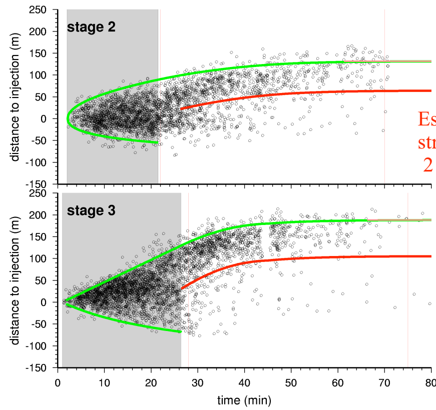

Estimated driving stress gradient:
$2 < g < 5$ MPa/km

Dahm et al., 2008

The 1979 Krafla (Iceland) rifting episode: example of lateral intrusions

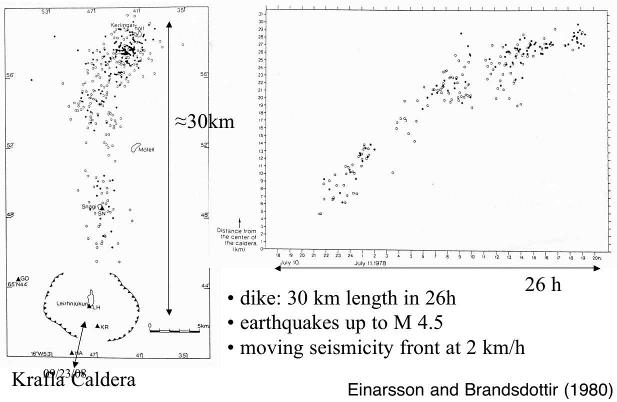

- dike: 30 km length in 26h
- earthquakes up to M 4.5
- moving seismicity front at 2 km/h

09/23/08

Einarsson and Brandsdottir (1980)

Application to the Krafla data

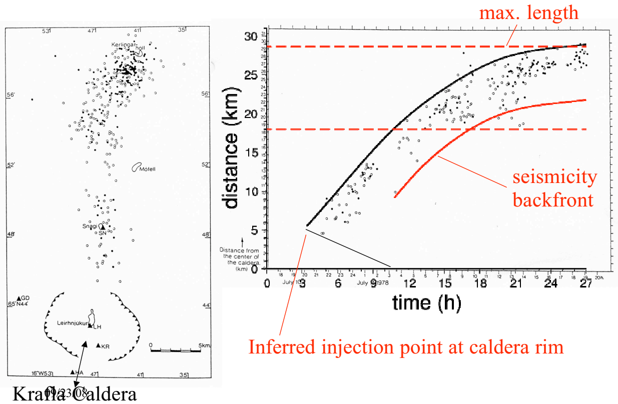

09/23/08

Fracture induced seismicity: conclusion

1. Fracture model explains injection-, transition and post-injection phase
2. Bilateral asymmetric and unilateral growth is explained
3. Pattern of induced seismicity correlates with regions of increased shear (Coulomb) stress
4. Front and back-front behaviour can be used to estimate stress gradients, overpressure and viscosity

Case III

Slow natural intrusions

Hydrofrac in plexiglas (Prof. F. Rummel)

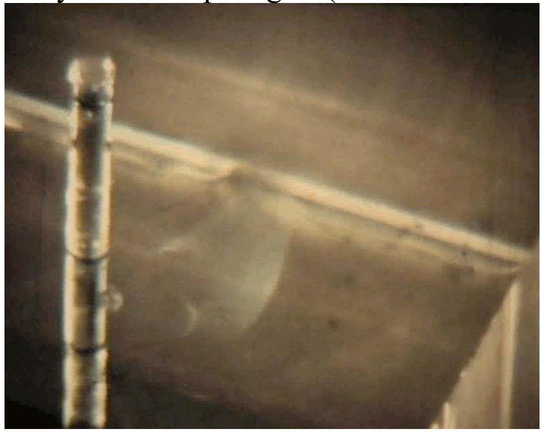

Hydrofrac in plexiglass

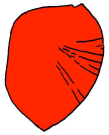

Hydrofrac in plexiglass

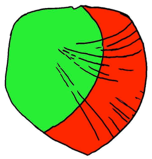

29

Hydrofrac in plexiglass

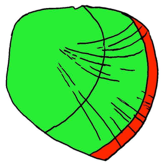

30

Hydrofrac in plexiglass

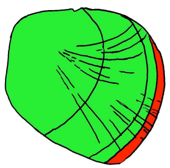

31

Hydrofrac in plexiglass

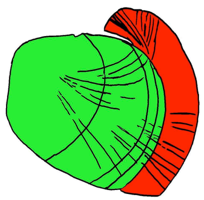

32

Hydrofrac in plexiglass

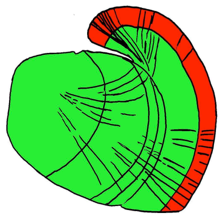

Hydrofrac in plexiglass

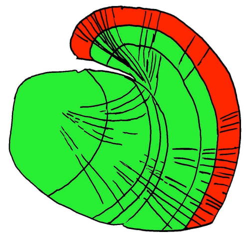

Hydrofrac in plexiglass

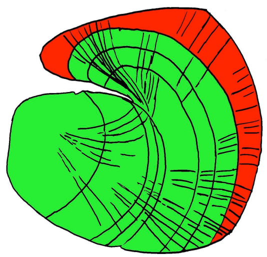

Hydrofrac in plexiglass

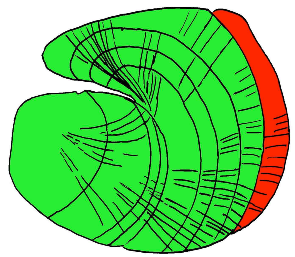

Hydrofrac in plexiglass

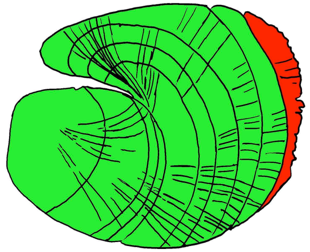

Example A: Izu Bonin Magma Intrusion Apr 2000

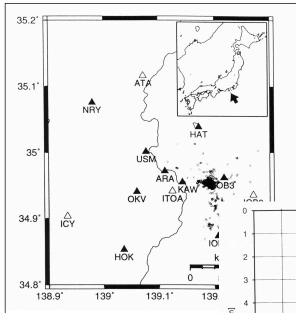

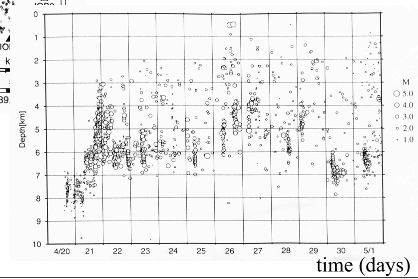

Hayashi & Morita (2002): A magma intrusion process inferred from hypocenter migration of earthquake swarms, GJI

Penny-shaped hypocenter pattern

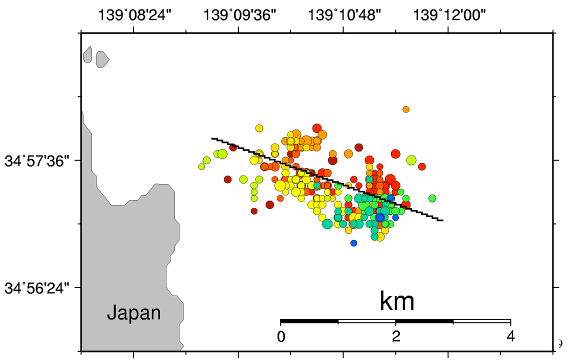

Penny-shaped hypocenter pattern

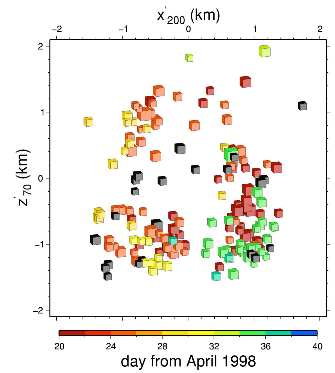

Penny-shaped hypocenter pattern

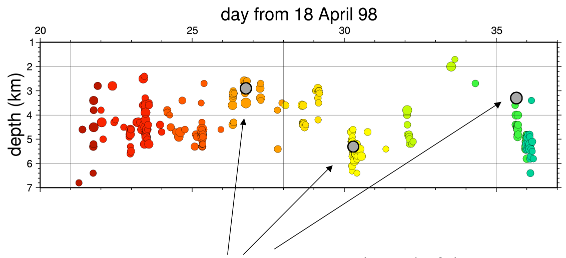

strongest events occur at the end of the sequence

maximal magnitudes ≈ M 4.5

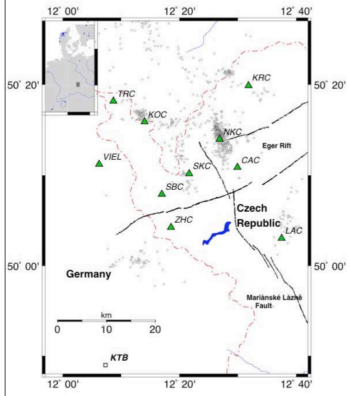

Example B: Earthquake swarm NW-Bohemia 2000

Xx events between …

Max M =

Hypo depth ≈ 8 km

"Weekly" migration of hypocenters

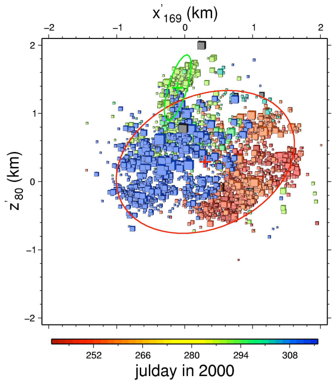

strongest events at the end of the sequence

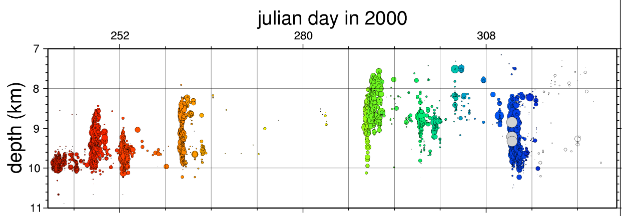

“scaling relations” of intrusion-induced seismicity ?

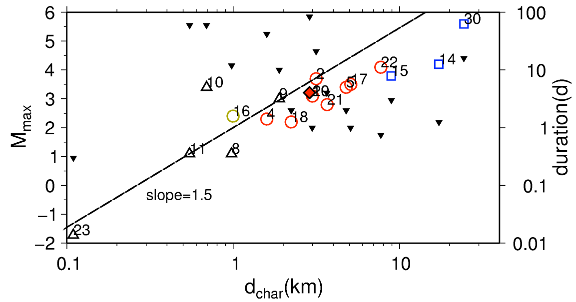

Dahm at al., (2008)

Elliptical crack develops under mixed loading

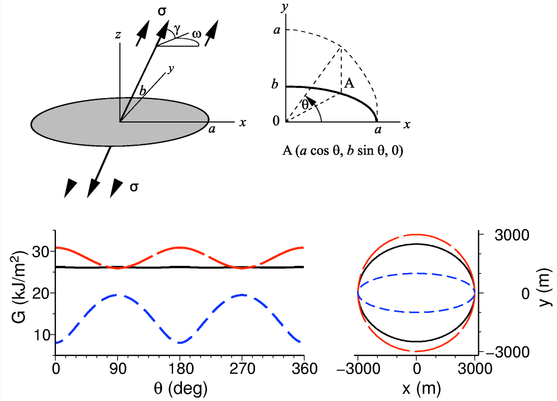

Dahm, Fischer and Hainzl (2008), in press

Summary of intrusion-induced seismicity

1. Fluid-filled fractures (non-buoyant) grow towards circular or elliptical final shape
2. The growth is episodic and discontinuous when the overpressure is small
3. The mechanics of growth seems to be similar for magma-dikes and for hydro-fractures
4. Earthquake magnitude scales with size of intrusion; largest events occur at the end of intrusion

Case IV

Gas field depletion

Trigger potential outside the reservoir

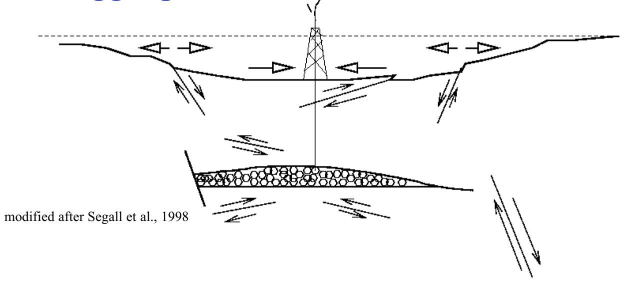

- Can distant earthquakes be triggered and what is mechanical evidence?
- Can seismic trigger potential be estimated ?

Seismicity close to gas field in N Germany and The Netherlands

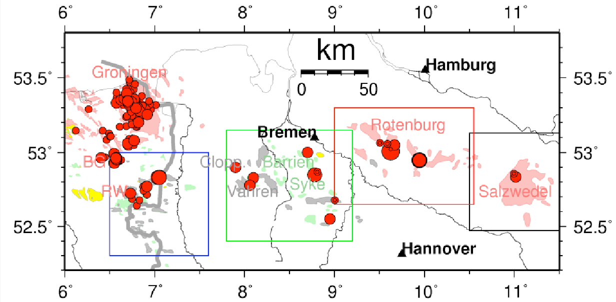

Was the Mw 4.4 Rotenburg 2004 earthquake related to gas-recovery?

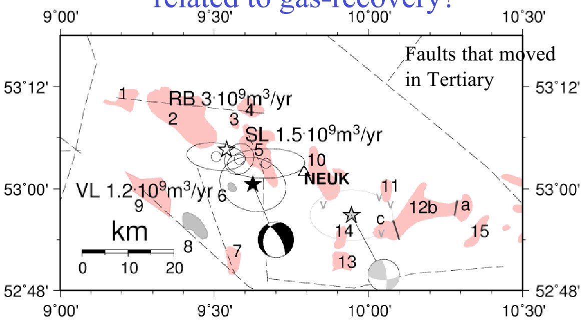

Gas-recovery is at a depth of 4.5-5 km, event depth at 5.1-6.4 km

Stress change from depletion of crack-reservoir

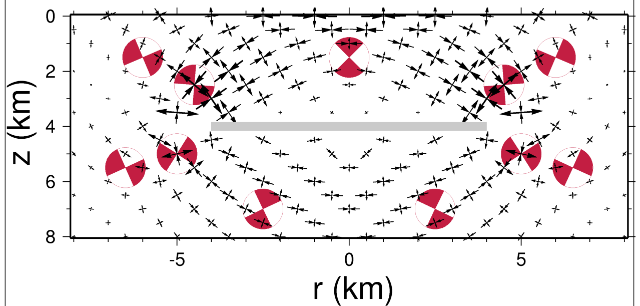

Modeling is based on a 3D Boundary Element method (in prep.)
Equivalent solutions are obtained from the Geertsma model (e.g. Segall, 1998)

Advantage of 3D-BEM method

1. fast calculation of displacement, deformation and stress
2. fields with complex shape can be handled
3. interaction of ‘fields’ is considered, e.g. fields at different depths intervals, neighbouring fields.
4. differential depletion can be analysed
5. field-fault interaction can be analysed

Predicted subsidence at Rotenburg fields

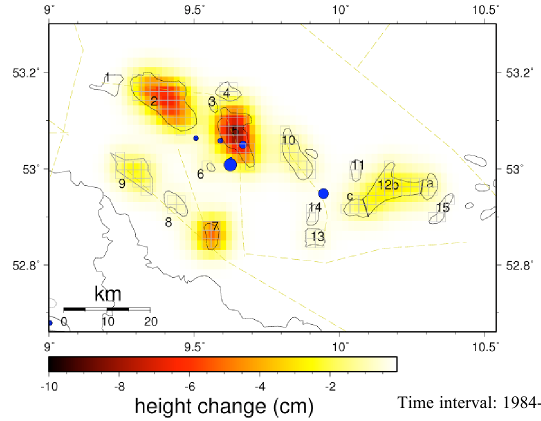

Time interval: 1984-2004

max. shear stress in 2004 in 6 km depth

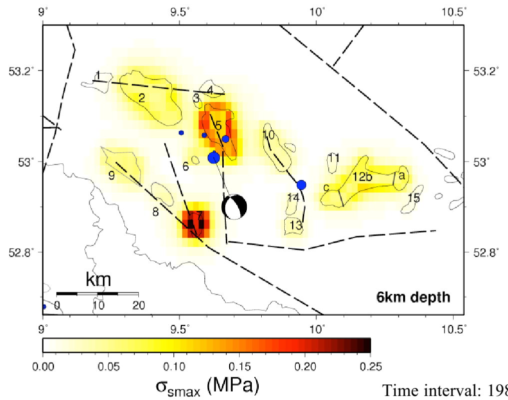

Time interval: 1984-2004

stress change in strike-dip-rake of 2004 event

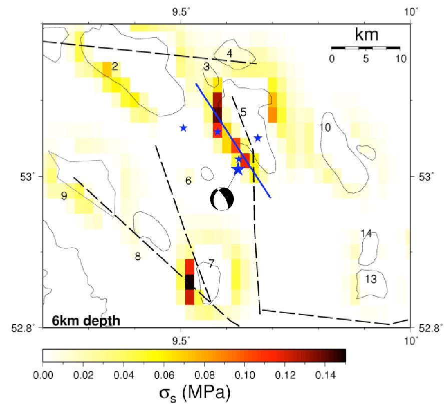

shear stress change on fault: vertical section

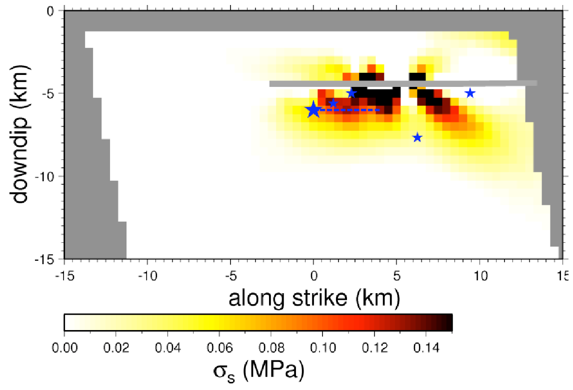

Conclusions

1. The Rotenburg earthquake occurred on a fault patch where shear and Coulomb stress increased as a result of field depletion
2. The stress increase was in the range of 0.1 MPa
3. The earthquake ruptured about 70% of the patch of increased stress on the fault, and no rupture outside the patch is indicated

Overall summary

1. Induced and triggered seismicity has many causes and is often difficult to distinguish from natural seismicity
2. It is not sufficient to correlate a loading cycle with earthquake statistical parameter. A time dependent stress model is needed to strengthen the trigger hypothesis
3. Natural fluid-induced seismicity can be used to study the intrusion parameter
4. Many tools are needed to study triggered and induced seismicity (relative location and depth studies, source mechanism, modeling of fluid diffusion, intrusion, depletion related stress changes)

references

Dahm, T. and Brandsdóttir, B., 1997. Moment tensors of micro-earthquakes from the Eyjafjallajökull volcano in South Iceland. Geophys. J. Int., 130:183–192.

Dahm, T., Fischer, T., and Hainzl, S., 2008a. Linear fracture growth during hydrofracturing: the role of driving stress gradients. Geophysics, 0(0):to be submitted.

Dahm, T., Fischer, T., and Hainzl, S., 2008b. Mechanical intrusion models and their constraints on the density of fluids injected in the nw bohemia swarm region at 10 km depth. Studia Geofisica, 0(0):in press.

Dahm, T., Krüger, F., Stammler, K., Klinge, K., Kind, R., Wylegalla, K., and Grasso, J., 2007. The $m_w = 4.4$ Rotenburg, Northern Germany, earthquake and its possible relationship with gas recovery. Bull. Seism. Soc. Am., 97(10.1785/0120050149):691–704.

Einarsson, P. and Brandsdóttir, B., 1980. Seismological evidence for lateral magma intrusion during the July 1978 deflation of the Krafla volcano in NE-Iceland. J. Geophys., pp. 160–165.

Fischer, T., Hainzl, S., and Dahm, T., 2008a. Asymmetric hydraulic fracture as a result of driving stress gradients. Geophys. J. Int., 0:submitted.

Fischer, T., Michalek, J., and Bouskova, A., 2008b. Microearthquake activity near Novy Kostel in the period 2001-2007: fault plane after a swarm. Studia Geophysica et Geodetica, 0:submitted.

Hayashi, A. and Morita, Y., 2003. An image of a magma intrusion process inferred from precise hypocentral migrations of the earthquake swarm east of the Izu Peninsula. Geophys. J. Int., 153:159–174.

Köhler, N., Spies, T., and Dahm, T., 2008. Seismicity patterns and variatoin of the frequency-magntiude distribution of microcracks in salt. Geophys. J. Int., x:submitted.

Seeber, L. and Armbruster, J., 2000. Earthquakes as bacons of stress change. Nature, 407:69–72.

Seeber, L., Armbruster, J., and Kim, W.-Y., 2004. A fluid-injection-triggered earthquake sequance in Ashtabalu, Ohio: Implications for seismogenesis in stable continental regions. Bull. Seism. Soc. Am., 94:76–87.

Segall, P. and Fitzgerald, S., 1998. A note on induced stress changes in hydrocarbon and geothermal reservoirs. Tectonophysics, 289:117–128.

Turcotte, D. and Schubert, G., 2002. Geodynamics, 2nd edition. 450, pp.